Microstructure and Thermal Stability of Ultra Fine Grained Mg-based Alloys Prepared by High Pressure Torsion

J. Čížek[1, a], I. Procházka[1], B. Smola[1], I. Stulíková[1], R. Kužel[1], Z. Matěj[1],
V. Cherkaska[1], R.K. Islamgaliev[2], O. Kulyasova[2]

[1]Faculty of Mathematics and Physics, Charles University,

V Holesovickach 2, CZ-18000 Praha 8, Czech Republic

[2]Institute of Physics of Advanced Materials, Ufa State Aviation Technical University,

Ufa 450000, Russia

[a]jcizek@mbox.troja.mff.cuni.cz

Abstract. In the present work we studied microstructure of ultra fine grained (UFG) pure Mg and UFG Mg-based alloys. The initial coarse grained samples were deformed by high pressure torsion (HPT) using pressure of 6 GPa. Such deformation leads to formation of UFG structure in the samples. The severe plastic deformation results in creation of high number of lattice defects. Therefore, we used positron annihilation spectroscopy (PAS) for defect characterizations. PAS represents a well developed non-destructive technique with high sensitivity to open volume defects like vacancies, vacancy clusters, dislocations etc. In the present work we combined PAS with TEM and XRD to obtain complete information about microstructure of the UFG samples studied. We have found that microstructure of HPT-deformed Mg contains two kinds of regions: (a) "deformed" regions with UFG structure (grain size 100-200 nm) and high number of randomly distributed dislocations, and (b) "recrystallized" regions with low dislocation density and grain size of few microns. It indicates some kind of dynamic recovery of microstructure already during HPT processing. On the other hand, homogenous UFG structure with grain size around 100 nm and high density of homogeneously distributed dislocations was formed in HPT-deformed Mg-9.33 wt.%Gd alloy. After characterization of the as-deformed microstructure the samples were subsequently isochronally annealed and the development of microstructure with increasing temperature and recovery of defects were investigated.

Introduction

Lightweight Mg-based alloys allow for a significant weight reduction in automotive and air industries and in structural applications. It leads to a lower consumption of the fossil fuels and other energetic sources. However, the applicability of Mg-alloys is limited due to their low melting temperature. A failure of the construction units can happen at temperatures higher than 100-200°C. There is a big effort in materials science to extend the applicability of Mg-alloys to higher temperatures. The particularly promising way is use of rare earth alloying elements [1]. For example Mg-Gd exhibits promising novel hardenable alloy with high creep resistance even at elevated temperatures [2]. Despite the favourable strength and thermal stability, a disadvantage of Mg-based alloys with rear earth elements consists in a low ductility, which is not sufficient for industrial applications. Thus, attempts to increase ductility of these alloys are highly desirable. Grain refinement is a well-known method how to increase ductility of metallic materials. It has been demonstrated that ultra fine grained (UFG) metals with grain size around 100 nm can be produced by high pressure torsion (HPT) [3]. A number of UFG metals exhibit favorable mechanical properties consisting in a combination of very high strength and a significant ductility. For this reason, it is highly interesting to examine microstructure and physical properties of UFG Mg-based light alloys. Following this purpose, microstructure investigations and defect studies of pure UFG

Mg and UFG Mg-Gd alloy were performed in the present work. Typical feature of UFG structure is a high number of defects introduced by severe plastic deformation. To characterize these defects we employed positron annihilation spectroscopy (PAS), which represents well developed non-destructive technique with high sensitivity to open volume defects [4]. PAS was combined with X-ray diffraction (XRD) and transmission electron microscopy (TEM).

Experimental

The specimens of Mg (technical purity) and Mg-9.33 wt.%Gd alloy (Mg10Gd) were studied. Note that Gd content is given in the weight percents. The alloy was prepared from the technical purity Mg by squeeze casting. The as-cast material was subjected to homogenization annealing at 500°C for 6 h followed by rapid quenching into water of room temperature. In addition, a well annealed high purity Mg (99.95 %) was used as a reference specimen. The UFG samples were prepared from the coarse grained initial materials by HPT at room temperature up to the true logarithmic strain e = 7 under high pressure of 6 GPa [3]. The HPT deformed samples were disk shaped with diameter 12 mm and thickness 0.3 mm. After characterization of the as-deformed microstructure, the samples were subjected to step-by step isochronal annealing (30°C / 30 min) from room temperature up to 500°C. Each annealing step was followed by rapid quenching and PL, TEM and XRD studies carried out at room temperature.

A fast-fast positron lifetime (PL) spectrometer similar to that described in [5] with timing resolution 170 ps (FWHM ^{22}Na) at the coincidence counts rate 120 s^{-1} was employed in the present work. A ^{22}Na positron source with activity 1.5 MBq sealed on 2 μm thick mylar foil was used. Decomposition of PL spectra into exponential components was performed using a maximum likelihood procedure [6]. TEM observations were performed by the JEOL 2000 FX electron microscope operating at 200 kV. XRD studies were carried out with the aid of XRD7 and HZG4 (Seifert-FPM) powder diffractometers using Cu K$_{\alpha}$ radiation.

Results and discussion

Pure Mg. The reference high purity Mg sample exhibits a single-component PL spectrum with lifetime τ_1 = 227 ps, see Table 1. It is in a reasonable agreement with calculated bulk positron lifetime τ_B in Mg [7]. On the other hand, PL spectrum of the as-received coarse grained Mg consists of two components listed in Table 1. The shorter component with the lifetime τ_1 comes from the free positrons while the longer one represents a contribution of positrons trapped at defects. The lifetime τ_2 of the longer component corresponds to positrons trapped at dislocations in Mg [7]. Thus, we conclude that positrons are trapped at dislocations introduced into the as-received Mg during casting and shaping. Dislocation density $\rho \approx 5 \times 10^{12}$ m^{-2} and the mean grain size of about 10 μm were estimated by TEM in this specimen. Typical TEM image of the coarse grained Mg sample is shown in Fig. 1a.

Table 1.Lifetimes and corresponding relative intensities of the exponential components resolved in PL spectra (except of the source contribution). The errors (one standard deviation) are given in parentheses.

Sample	τ_1 [ps]	I_1 [%]	τ_2 [ps]	I_2 [%]
high purity Mg, well annealed	227.0(5)	100	-	-
Mg as-received	204(4)	63(1)	256(1)	37(1)
Mg10Gd, homogenized	220(4)	90.9(6)	301(9)	9.1(7)
HPT Mg	188(5)	39(1)	257(3)	61(1)
HPT Mg10Gd	210(3)	34(2)	256(3)	66(2)

A representative TEM image of the HPT-deformed Mg specimen is shown in Fig. 1b. Two different kinds of regions were observed: i) "deformed regions" with UFG grains (100-300 nm) and a high dislocation density, and ii) "recrystallized regions" with substantially larger grains ($\approx$ 1 µm) and almost free of dislocations. The presence of the "recrystallized regions" indicates some kind of dynamic recovery of microstructure during the HPT processing. The XRD back-reflection pattern is a superposition of isolated spots and continuous diffraction rings, which testifies co-existence of the two kinds of regions. The sample shows a texture of (001) type. The PL spectrum of the HPT deformed Mg consists of the free positron component and a contribution of positrons trapped at dislocations inside the "deformed region".
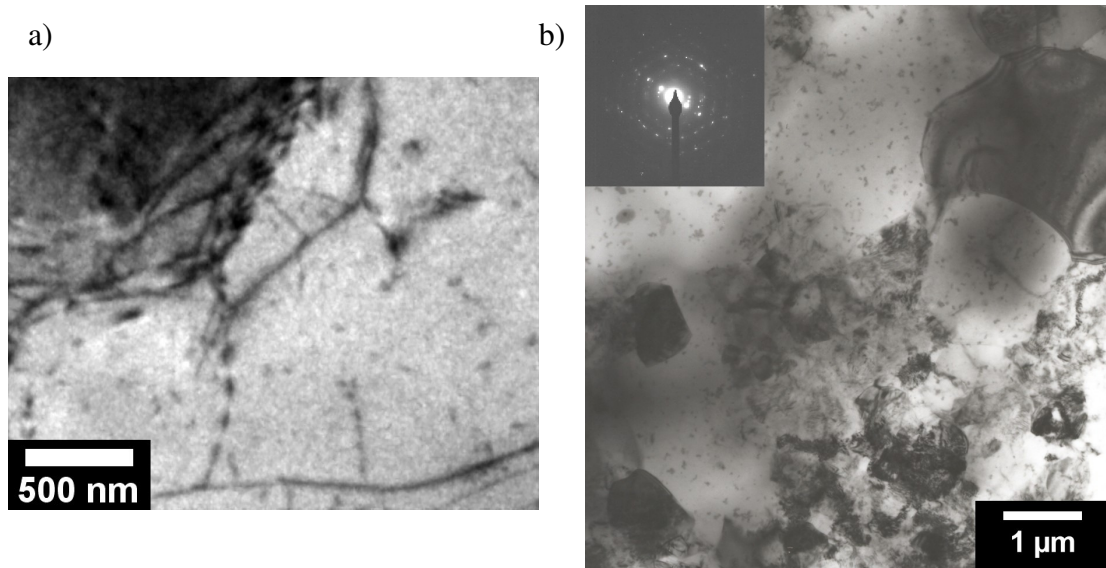

Figure 1. Typical TEM image of (a) coarse-grained Mg sample and (b) HPT-deformed Mg sample.
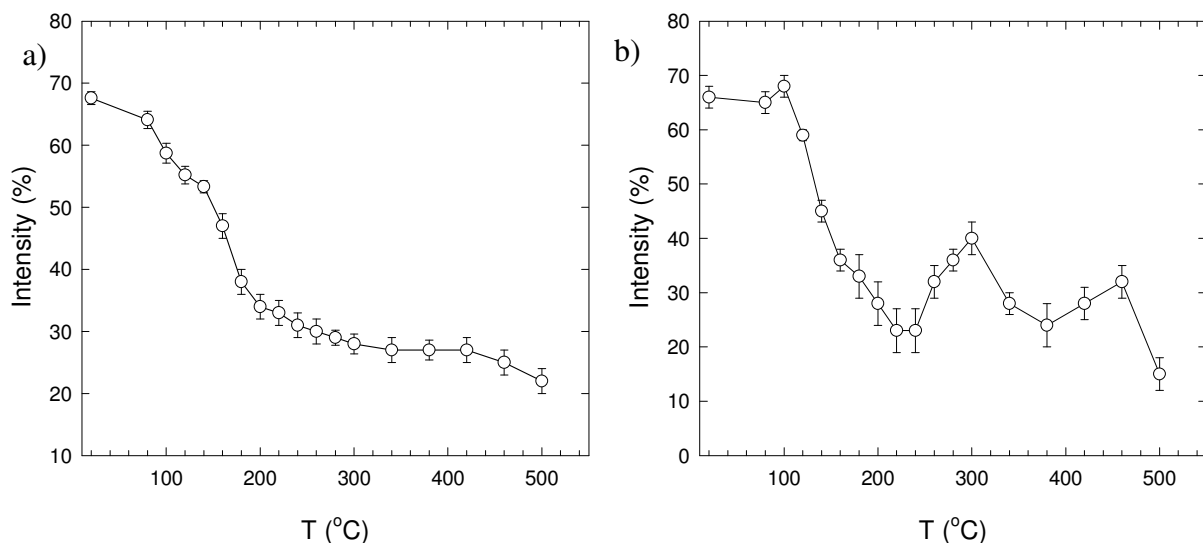

Figure 2. Temperature dependence of the relative intensity I_2 of positrons trapped at defects (a) HPT-deformed Mg (b) HPT-deformed Mg10Gd.

As the next step we investigated thermal evolution of microstructure of HPT deformed Mg. It was found that PL spectra of HPT-deformed Mg sample were well fitted by two exponential components at all annealing temperatures. The lifetime τ_2 of trapped positrons does not depend on

temperature and exhibits only a random scatter around the value of 256 ps corresponding to trapping at dislocations in Mg. The relative intensity I_2 of trapped positrons is plotted in Fig. 2a as a function of annealing temperature. It exhibits a strong decrease in the temperature range from $80\,^{\circ}C$ to $200^{\circ}C$ indicating recovery of dislocations. TEM observations revealed that "deformed regions" with UFG structure and high dislocation density are gradually replaced by the "recrystallized regions". Above $200^{\circ}C$ the sample exhibits recrystallized grains with mean size around 5 μm and the mean dislocation density falls below $\approx 10^{12}$ m^{-2}. A TEM image of the sample annealed at $200^{\circ}C$ is shown in Fig. 3a. It should be noted that there still remains a contribution of trapped positrons with intensity $I_2 \approx 20\%$ at temperatures above $300^{\circ}C$. It comes most probably from positron trapping at vacancy-like defect at grain boundaries.
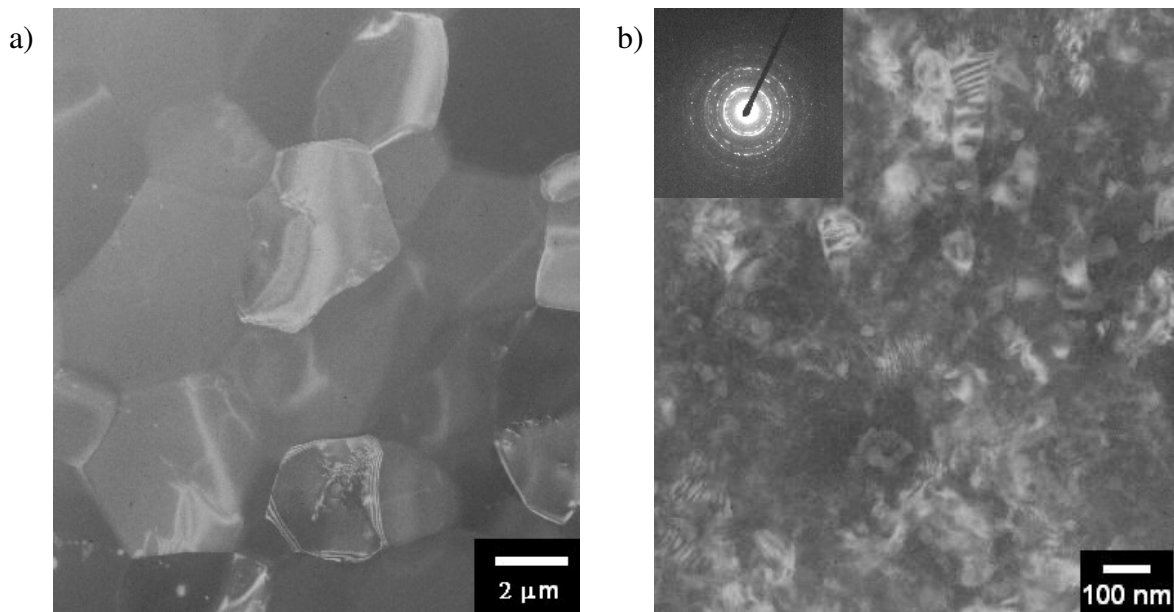

Figure 3. Bright-field TEM image of (a) HPT-deformed Mg annealed up to $200^{\circ}C$ (b) HPT-deformed Mg10Gd annealed up to $220^{\circ}C$.

Mg10Gd alloy. A bright-field TEM image of the homogenized Mg-10%Gd alloy is shown in Fig. 4a. Large coarse grains and a low dislocation density below $\approx 10^{12}$ m^{-2} were found by TEM. The PL spectrum of this specimen is well fitted by two exponential components given in Table 1. The first component with the lifetime τ_1 can be attributed to free positrons, while the second one with the lifetime τ_2 comes from positrons trapped at defects. The low dislocation density in the specimen approaches the lower sensitivity limit of PL spectroscopy [4]. Therefore, positrons trapped at dislocations cannot represent a noticeable contribution to PL spectrum. The second component with the lifetime τ_2 represents a contribution of positrons trapped in quenched-in excess vacancies, which were "frozen" in the sample due to the rapid quenching. This interpretation is supported by the lifetime $\tau_2 \approx 300$ ps, which is remarkably higher than the lifetime 256 ps of positrons trapped at dislocations in Mg, and agrees well with the calculated lifetime of positrons trapped at monovacancy in Mg. Monovacancies in pure Mg become mobile below room temperature [8]. Thus, free Mg monovacancies quickly disappear during and/or after quenching. Contrary to it, we observed that positrons are trapped in the monovacancies in the homogenized Mg10Gd sample. The explanation is that the monovacancies are bound to Gd atoms. The vacancy-Gd pairs are stable at room temperature. Indeed, an enhanced amount of Gd in the vicinity of vacancies was proved by coincidence Doppler broadening measurements [9].

A typical TEM image of HPT-deformed Mg10Gd alloy is shown in Fig. 4b. It shows uniform UFG microstructure with the mean grain size about 100 nm, i.e. contrary to pure Mg no dynamic recovery took place during the HPT processing. The electron diffraction pattern testifies high-angle missorientation of neighboring grains. A high density of homogeneously distributed dislocations was observed. From TEM observations one can estimate dislocation density $\rho \geq 10^{14}$ m^{-2}. The high dislocation density is reflected also by a significant broadening of XRD profiles. A lower broadening of (00l) profiles with respect to other peaks indicates a dominating presence of (00l) dislocations with Burgers vector $\vec{b}$ = $1/3.a.[2\bar{1}\bar{1}0]$. A weak (001) texture was found. The PL spectrum of the HPT-deformed Mg10Gd alloy consists of two components, see Table 1. The first component with the lifetime τ_1 comes from free positrons. The lifetime τ_2 of the second component corresponds well with that of positrons trapped at dislocations in Mg. One can see in Table 1 that I_2 is comparable for both HPT-deformed samples despite the fact that HPT-deformed Mg-10%Gd alloy exhibits obviously remarkably higher dislocation density. A possible explanation of this surprising effect is that contrary to pure Mg, the Mg10Gd alloy contains predominantly partial dislocations, which exhibit reduced specific positron trapping rate, i.e. their capability of positron trapping is lower compared to dislocations in Mg [9].
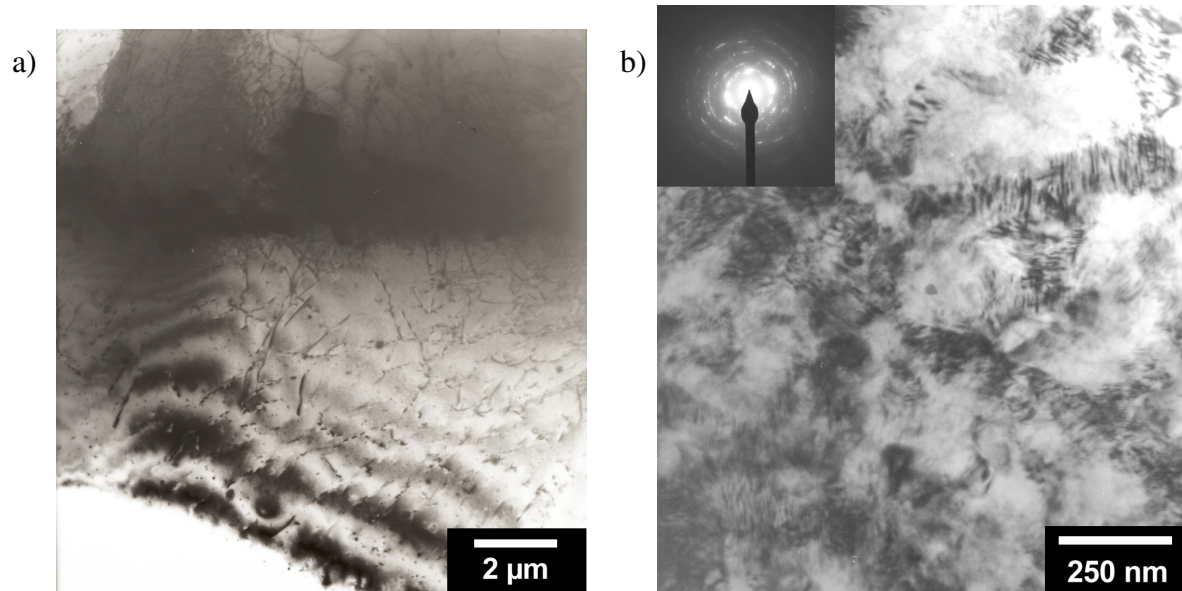

Figure 4. Typical TEM image of (a) coarse-grained (homogenized) Mg10Gd sample and (b) HPT-deformed Mg10Gd alloy

Thermal development of microstructure of coarse grained Mg10Gd alloy was studied in details in Refs. [2,7]. Homogenized Mg-10%Gd alloy represents a supersaturated solid solution (sss). With increasing temperature it decomposes in the following sequence: sss $\rightarrow$ β'' ($D0_{19}$) metastable $\rightarrow$ β' (c-bco) metastable $\rightarrow$ β (fcc) stable. In the present work we describe thermal evolution of UFG microstructure of HPT-deformed Mg-10%Gd. It was found that PL spectra of this sample are well fitted by two components for all the annealing temperatures. Similarly to HPT-deformed Mg, the lifetime τ_2 exhibits only a random scatter around the value for dislocations in Mg. Temperature dependence of the relative intensity I_2 of trapped positrons is plotted in Fig. 2b. One can see that I_2 exhibits a dramatic decrease in the temperature interval from $100^{\circ}C$ to $220^{\circ}C$. It corresponds to recovery of dislocations. The mean dislocation density decreased almost by one order of magnitude in this temperature range. However, no grain growth was observed by TEM in the sample annealed up to $220^{\circ}C$. A bright-field TEM image of the sample annealed up to $220^{\circ}C$ is shown in Fig. 3b. One can see in the figure that grain size remains still around 100 nm. Contrary to coarse grained

alloy, the metastable phases do not precipitate in HPT-deformed Mg10Gd. Precipitation of fine particles (diameter $\leq$ 100 nm) of the stable β phase was observed from 260°C. Note that precipitation of the β phase in coarse grained Mg-10%Gd starts only at 400°C [2]. The Gd-rich β phase precipitates are not coherent with Mg matrix. Precipitation of β phase leads, therefore, to creation of new open-volume defects at precipitate-matrix interfaces. Positron trapping at these defects is reflected by an increase of the intensity I_2 above 240°C with a local maximum at 300°C. At higher temperatures coarsening of the β phase precipitates takes place followed by their dissolution and restoration of solid solution.

Summary

Microstructure of HPT-deformed Mg and Mg10Gd was characterized and compared with initial coarse grained materials. An incomplete dynamic recovery took place during HPT processing of Mg sample which resulted in a binomial type of structure. The HPT-deformed Mg10Gd exhibits homogeneous UFG microstructure with high density of uniformly distributed dislocations and grain size about 100 nm. Recovery of dislocations took place in the temperature range from 100°C to 220°C in both HPT-deformed samples. In case of HPT-deformed Mg the regions with UFG structure and high density of dislocations are replaced by recrystallized grains. On the other hand, recovery of dislocations in HPT-deformed Mg10Gd is not connected with any grain growth and the sample annealed up to 260°C exhibits still grain size around 100 nm. Precipitation effects in HPT-deformed Mg-10%Gd sample differ significantly from that in coarse grained alloy, namely: (i) the metastable phases do not precipitate, (ii) the β phase particles are finer and precipitate at substantially lower temperatures.

Acknowledgement

References

[1] B.L. Mordike, Mat. Sci. Eng. A Vol. 324 (2002), p. 103.

[2] P. Vostrý, B. Smola, I. Stulíková, F. von Buch, B.L. Mordike, phys. stat. sol. (a) Vol. 175 (1999), p. 491.

[3] R.Z. Valiev, R.K. Islamgaliev, I.V. Alexandrov, Prog. Mat. Sci. Vol. 45 (2000), p. 103.

[4] P. Hautojärvi, C. Corbel, in: Proceedings of the International School of Physics "Enrico Fermi", Course CXXV, Ed. A. Dupasquier, A.P. Mills, IOS Press, Varena (1995), p. 491.

[5] F. Bečvář, J. Čížek, L. Lešťak, I. Novotný, I. Procházka, F. Šebesta, Nucl. Instr. Meth. A Vol. 443 (2000), p. 557.

[6] I. Procházka, I. Novotný, F. Bečvář, Mat. Sci. Forum Vol. 225-257 (1997), p. 772.

[7] J. Čížek, I. Procházka, F. Bečvář, I. Stulíková, B. Smola, R. Kužel, V. Cherkaska, R.K. Islamgaliev, O. Kulyasova, Acta Materialia, (2005) submitted for publication.

[8] M. Fahnle, B. Meyer, J. Mayer, J.S. Oehrens, G. Bester, in: Diffusion Mechanisms in Crystalline Materials, Ed. Y. Mishin, MRS Symposia Proceedings No. 527, p. 23.

[9] J. Čížek, I. Procházka, F. Bečvář, I. Stulíková, B. Smola, R. Kužel, V. Cherkaska, R.K. Islamgaliev, O. Kulyasova, Acta Physica Polonica A, (2005) in print.